Numerical Simulation of Industrial-Scale Fluidised Bed Reactors Using an Artificial Neural Network EMMS Drag Model

P Stamatopoulos[1], G Kanellis[1], T Lyras[1], D Stefanitsis[1] and N Nikolopoulos[1]

[1]Chemical Process & Energy Resources Institute, Centre for Research and Technology Hellas (CERTH), 52 Aigialias street, 15125, Athens, Greece

Abstract. This work presents an Artificial Neural Network Energy Minimization Multi-Scale (ANN-EMMS) drag scheme specifically developed for fluidised bed reactors of chemical looping combustion (CLC) applications. The data that feed the neural network are generated by a custom-built MATLAB code that solves the EMMS equations for gas-particle conditions corresponding to those encountered in CLC. The presented ANN-EMMS model is trained for a wide range of operating conditions, including different particle properties and reactor diameters. The examined particles correspond to CLC bed materials, namely ilmenite ($FeTiO_3$), hematite (Fe_2O_3) and titanium oxide (TiO_2). The ANN-EMMS model's performance is validated against numerical data produced using the conventional EMMS model, showing excellent agreement. To demonstrate the model's performance, an industrial-scale fluidised bed reactor is numerically investigated for two modes of operation, firstly in a co-fired mode and secondly as a retrofitted air reactor. The results from the co-combustion operation are compared against experimental measurements, while in the case of the air reactor, the results are compared against 1D dynamic process modelling results. A significant advantage of the ANN-EMMS model is that, unlike the conventional scheme, it takes into account a larger number of different properties in the induced flow field. Additionally, it can be used for various numerical parametric studies without any modification. Thus, the developed ANN-EMMS model can substantially reduce the need for pre-processing computational resources and, eventually, accelerate numerical investigations that focus on the design and operation optimisation of fluidised bed reactors, as well as on the utilisation of different inert materials.

Keywords: Artificial Neural Network; Energy Minimization Multi-Scale drag scheme; Chemical Looping Combustion

1. Introduction

The conventional energy-minimization multi-scale (EMMS) drag model takes into account the mesoscale structural effect when calculating the drag coefficient in each computational cell [1]. Heterogeneity is represented by a heterogeneity index $H_d = F_{Wen\&Yu}/F_{EMMS}$ which is obtained from analytical, empirical, and semi-empirical equations [2,3]. The EMMS model is based on the principle that gas-solid interactions in a fluidized bed minimize net energy transfer, reflecting the system's tendency to follow paths with the least pressure drop as gas flows through solids. However, EMMS models primarily target monodisperse flows, as they relate the heterogeneity index, H_d, to local gas properties without accounting for variations in particle diameter. In contrast to the traditional EMMS model, the proposed Artificial Neural Network (ANN) EMMS model establishes a correlation between the heterogeneity index and seven operating parameters, as well as a dimensionless velocity, ¯, defined as the ratio of slip velocity to terminal velocity, which enables the model to be applied to simulations involving particles with varying properties. Artificial neural networks have been used in several studies to develop more general EMMS drag models taking into account different particle properties and operating conditions [4,5]. The advantage of the present model is that the neural network was trained under an extensive range of operating conditions, providing adequate resolution on drag calculations that affect the accuracy of the simulation, particularly in multi-dispersed flows, thus improving the model performance while reducing overall computational cost. This study, presents the training of an ANN-EMMS model for the prediction of H_d, based on particle properties and reactor diameter, and its use for the numerical investigation of a circulating fluidized-bed (CFB) unit, in two operating modes.

2. Methodology

The neural network presented in this work was developed using the Neural Net Fitting Matlab application. The fitting network was trained using the Levenberg-Marquardt (LM) algorithm [6]. This algorithm is

*Corresponding Author, P. Stamatopoulos stamatopoulos@certh.gr

specifically designed to minimize the sum of squared error functions by updating the values of weights and bias and is the fastest backpropagation algorithm in the Matlab toolbox, as it does not require the computation of the Hessian matrix. **Figure 1** illustrates the neural network structure, where the input layer consists of seven parameters, i.e. particle diameter, d_p, gas phase viscosity, μ_g, gas phase density, ρ_g, gas phase voidage, ε_g, solid phase density, ρ_s, reactor diameter, D_r and dimensionless velocity, $\bar{}$, the hidden layers process weighted inputs using a sigmoid activation function and the output layer generates the heterogeneity index, H_d.

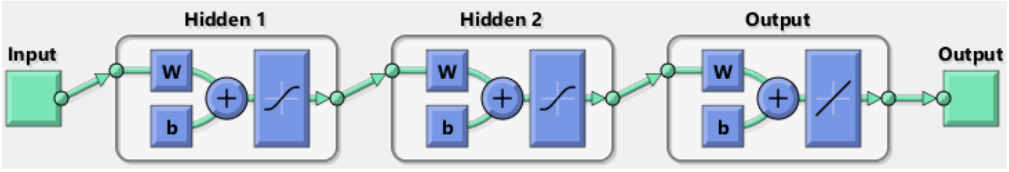

Figure 1. Graphical diagram of the developed neural network.

To train the ANN-EMMS model, raw data are needed. This data should correspond to various particle properties relevant to the co-combustion and air reactor operations. For this purpose, 24 cases with varying parameter combinations were carefully selected. A conventional EMMS build-in code [7] was utilised for the numerical simulations and the initial dataset generated comprised approximately 310,500 points. From a total of 24 cases, 22 cases were used for the training of the neural network and two cases were used for the validation of the ANN-EMMS prediction. The accuracy of ANN models depends on the training datasets and is influenced by the diversity, quality, and quantity of the available data. Moreover, the datasets must span the entire input space. To this end, new data points were generated through interpolation to enhance coverage, increasing the number of points for training, validation and testing of the ANN-EMMS to 6,369,000. To simplify training, the data were divided into three gas voidage classes (ε_g between 0.65 and 0.82, 0.82 and 0.95, and 0.95 and 1) leading to the development of three separate networks, ANN-a, -b and –c, as presented in **Figure 2**. In order to increase the accuracy of each artificial neural network, parametric studies were performed in order to define the optimal number of hidden layers and the number of neurons. It is worth mentioning that each time a neural network is trained, it can result in a different solution due to random initialization of weight, bias values and a different division of data input into training, test, and validation sets. Thus, 10 individual retrains were carried out to obtain the best network training result. **Table 1** shows information on each neural network, i.e. number of hidden layers, number of neurons at each layer and the performance metrics, such as the mean absolute percentage error (MAPE), the coefficient of determination, R^2 and the linear regression coefficients. Finally, the accuracy of the ANN was tested using the data from cases 23 and 24, which were not included in the training. In case 23 the MAPE was less than 14.5%, while in case 24 the average MAPE was less than 13.5%.

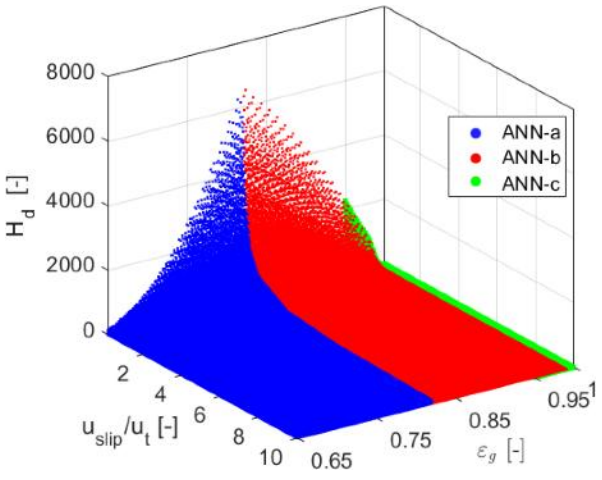

Figure 2. Training datasets, for ANN-a (blue), ANN-b (red) and ANN-c (green).

*Corresponding Author, P. Stamatopoulos stamatopoulos@certh.gr

Table 1. Information and performance metrics of ANN neural networks.

ANN	Number of neurons		MAPE [%]	R^2	y = a·x + b	
	1st layer	2st layer			a	b
ANN-a	17	14	19.32%	0.998	1	0.022
ANN-b	17	8	19.2%	0.999	1	0.03
ANN-c	14	19	14.07%	0.993	1	0.26

The design specifications of the commercial CFB boiler, provided by FORTUM and SFW, are presented in **Figure 3(a)**. The unit measures 34 m in height (z-axis), 12 m in width (y-axis), and 5.2 m in depth (x-axis). The height of the upper furnace is 28 m. The reactor outlet is a 9 m by 1 m rectangle positioned at z = 24.5 m. The complete numerical domain is depicted in **Figure 3(b)**. Due to its X-Z plane symmetry, only half of the domain was considered for reduced computational cost. The lower furnace can be seen in **Figure 3(c)** and it has a height of 6 m. The primary air inlet is a 3.5 m by 12 m rectangle located at the lower furnace's bottom. Eight secondary air inlets of 0.2 m hydraulic diameter are placed at heights of 0.5 m and 2.0 m. Two rectangular inlets, 0.8 m by 3.5 m, allow solid recirculation from the separator legs. On the opposite side, as shown in **Figure 3(d),** the square-shaped fuel inlet has a side of 0.8 m and is located at z = 0.75 m. The above-described domain was used for both numerical investigations presented in this work.

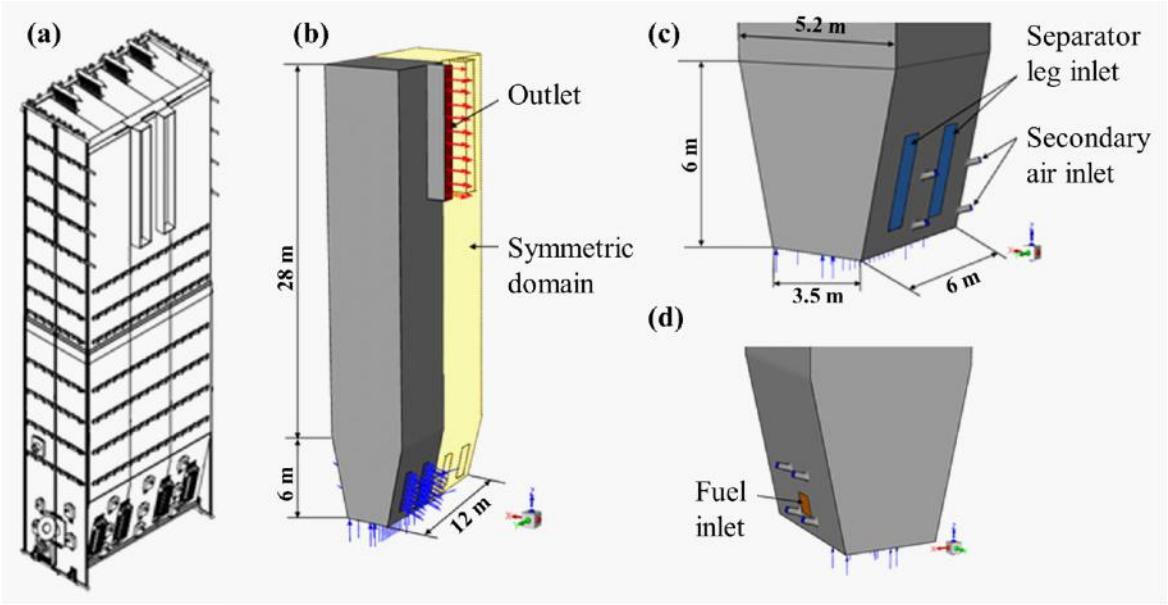

Figure 3. Industrial CFB boiler (a), the corresponding numerical domain (b) and details of the lower furnace including primary and secondary air inlet, and separator leg inlet (c) and fuel inlet (d).

Regarding the operation of the unit in co-combustion mode, the boundary conditions of the numerical investigation are presented in **Table 2**. The fluidization gas entering from the primary and secondary inlet has a constant temperature of 463.15 K and 483.15 K, respectively. The mass flow rate of air supplied from the primary inlet (bottom) is 26.81 kg/s, while the eight secondary inlets have a combined mass flow rate of 16.73 kg/s. At the outlet, the pressure is assumed to be atmospheric, with a backflow temperature of 1160 K. The model includes three types of solid materials: inert ash, and fuel consisting of Solid Recovered Fuel (SRF) and coal particles. At the lower part of the vessel, a square inlet is defined as a mass-flow inlet, where SRF and coal fuels are injected with a constant mass flow rate of 3.5 kg/s at 293.15

*Corresponding Author, P. Stamatopoulos stamatopoulos@certh.gr

K for SRF, and 2.25 kg/s at 303.15 K for coal. On the opposite side of the SRF inlet, the separator leg is located. Through this opening, the bed material that leaves the outlet is re-entering the domain with the use of a user-defined function.

Table 2. Boundary condition for unit operation operation in co-combustion mode.

Boundary	Type	gas		solid		
		$\dot{}$ [kg/s]	Temp [K]	fuel	$\dot{}$ [kg/s]	Temp [K]
primary inlet	mass flow inlet	26.81	463.15	-	-	-
secondary inlet	mass flow inlet	16.73	483.15	-	-	-
SRF inlet	mass flow inlet	0.001	300	SRF	3.5	293.15
				Coal	2.25	303.15
separator leg inlet	mass flow inlet	0.001	1160	Bed material	Recirculation via UDF	
outlet	pressure outlet	-	1160		Recirculation via UDF	

Regarding the operation of the unit as an air reactor (AR), the boundary conditions are presented in **Table 3.** In this mode, the secondary inlets are not operational and are treated as walls. Air enters from the preheater at 473.15 K with a mass flow rate of 57.35 kg/s. Fresh oxygen carrier (OC) particles, including ilmenite and char, are injected through the SRF inlet. Ilmenite enters at 298.15 K with a mass flow rate of 3.45 kg/s, while char enters at 1213.15 K with a flow rate of 0.054 kg/s. Circulation of OC from the fuel reactor is introduced through the separator inlet using a user-defined function. To accelerate the reaching of a quasi-steady-state condition, 36.4 tons of initial ilmenite particles are introduced into the furnace, consisting of 11.5% ilmenite, 44.25% hematite, and 44.25% titanium dioxide. To manage heat from the exothermic OC regeneration process, a total heat flux of 17.45 MW is applied to the side walls for cooling.

Table 3. Boundary conditions for unit operation as an air reactor.

Boundary	Type	gas		solid		
		$\dot{}$ [kg/s]	Temp [K]	fuel	$\dot{}$ [kg/s]	Temp [K]
primary inlet	mass flow inlet	57.35	463.15	-	-	-
SRF inlet	mass flow inlet	0.001	300.15	ilmenite &	3.45	298.15
				char	2.25	303.15
separator leg inlet	mass flow inlet	0.001	1160	Circulating ilmenite	circulation via UDF	1213.15
outlet	pressure outlet	-	1273.15		circulation via UDF	

3. Results

The simulation in co-combustion mode is unsteady and assumes isothermal conditions, which aligns with the measured temperature profile. The solution process is divided into two parts: the first part lasts for 110 seconds, during which the system approaches a pseudo-steady state in terms of species concentrations at the reference (outlet) surface. Subsequently, the second part, lasting 40 seconds, is initiated. During this part, data sampling is enabled, and time-averaged quantities are obtained, which are used as a reference or comparison against measurement data. **Figure 4** compares the simulated and measured pressure profiles, averaged over 40 seconds, at seven heights along the reactor. The simulation shows strong agreement with

*Corresponding Author, P. Stamatopoulos stamatopoulos@certh.gr

experimental data, with the mean pressure drop closely matching measurements and a total average percentage error equal to 10.78%. The numerically calculated pressure value close to the inlet, at a height of 0.3 m was 3709 Pa, 5.17 % lower than the corresponding experimental value. **Table 4** presents the average mass fractions of species at the reactor outlet, with the simulation predicting an O_2 mass fraction of 4.77%, compared to the experimental value of 5.6%, resulting in a deviation of 14.82%. **Table 5** provides time-averaged flow rates for gas and solid phases. With regard to the simulation of the air reactor, the initial OC particle composition consists of 11.5% $FeTiO_3$, 44.25% Fe_2O_3, and 44.25% TiO_2. As ilmenite oxidizes, $FeTiO_3$ converts into Fe_2O_3 and TiO_2, reaching a pseudo-steady state after 90 seconds. Time-averaged data is collected over the next 40 seconds, where the pressure stabilizes at 12,600 Pa at 0.3 m, corresponding to 37.28 tons of fuel inside the reactor.

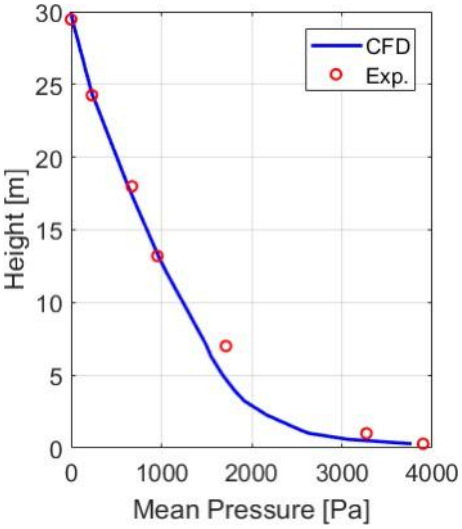

Figure 4. Time-averaged pressure drop along the reactor height.

Table 4. Mean mass fraction values at the outlet surface.

Species	Mean mass fraction [%]
O_2	4.77 - numerical
	5.6 - experimental
H_2O	6.67
CO_2	18.84
SO_2	0.078
Cl_2	0.044
CO	1.70E-04
Volatiles SRF	8.35E-05
Volatiles Coal	1.40E-05
N_2	69.60
SUM	100

Table 5. Mean mass flow rate of the gas and solid phase at the outlet of a full-scale unit.

Phase	Mean mass flow rate [kg/s]
Solid	631.6
gas	97.25
Species	
O_2	3.72
H_2O	6.78
CO_2	19.22
SO_2	0.08
Cl_2	0.046
CO	6.50E-04
Volatiles SRF	3.14E-04
Volatiles Coal	1.45E-05

Table 6 compares the results of the CFD simulation with those from a 1D process modelling software, showing a deviation equal to 1.8% in gas phase mass flow rates and 0.8% in the outlet temperatures. Regarding the mass flow rate of the solid phase, the CFD-predicted values are higher by 16.05% compared to the 1D model predictions, which can be attributed to the more accurate representation of the flow field and particle trajectories inside the reactor by the transient 3D CFD model as opposed to the 1D steady-state process modelling.

*Corresponding Author, P. Stamatopoulos stamatopoulos@certh.gr

Table 6. Comparison between 1D process modelling and CFD simulation results.

	Process modelling	**CFD**	**Deviation [%]**
Outlet gas phase			
Mass flow rate [kg/s]	100.307	102.076	1.8%
Temp [K]	1273.15	1283.45	0.8%
O_2 [%]	10.60	11.31	6.7%
CO_2 [%]	0.30	0.25	-6.8%
N_2 [%]	89.10	88.44	-0.7%
Outlet solid phase			
Mass flow rate [kg/s]	721.744	837.56	16.05%
$FeTiO_3$ [%]	6.2	7.16	15.4%
Fe_2O_3 [%]	46.9	46.42	-1.02%
TiO_2 [%]	46.9	46.42	-1.02%

4. Conclusions

An artificial neural network EMMS drag model was developed and used for the simulation of an industrial circulating fluidised bed unit operating in two distinctive modes. The first mode was a co-combustion mode, where the unit was operated as a combustor fuelled by a combination of SRF and coal particles. In the second mode, the unit operated as an air reactor, where the oxygen carrier particles would be regenerated in an oxygen-rich state. Along with the in-house ANN-EMMS drag model, the simulations utilised a dense discrete phase model (DDPM) approach, available with the ANSYS Fluent software. The ANN-EMMS model accurately predicted drag forces without additional training time, demonstrating strong agreement with both co-combustion experimental data and air reactor process modelling results. More specifically, for co-combustion operation, the average pressure drop deviation compared to experimental measurements was 10.78%, while in air reactor operation a deviation of 0.8% is found in the estimation of outlet gas temperature and a deviation of less than 7% in the prediction of gas species concentrations. However, the main advantage of the artificial neural network approach is that in both numerical investigations, the drag force was calculated using the same ANN-EMMS model, thus avoiding a time-consuming pre-processing step. Especially, in the case of extended, multi-parametric numerical campaigns, the benefit of the ANN approach is substantial.

5. References

[1] Wang J, Ge W and Li J 2008 Eulerian simulation of heterogeneous gas–solid flows in CFB risers: EMMS-based sub-grid scale model with a revised cluster description *Chem. Eng. Sci.* **63** 1553–71
[2] Ghadirian E and Arastoopour H 2016 CFD simulation of a fluidized bed using the EMMS approach for the gas-solid drag force *Powder Technol.* **288** 35–44
[3] Li J, Huang W, Chen J, Ge W and Hou C 2018 Mesoscience based on the EMMS principle of compromise in competition *Chem. Eng. J.* **333** 327–35
[4] Zhu L-T, Chen X-Z, Ouyang B, Yan W-C, Lei H, Chen Z and Luo Z-H 2022 Review of Machine Learning for Hydrodynamics, Transport, and Reactions in Multiphase Flows and Reactors *Ind. Eng. Chem. Res.* **61** 9901–49

*Corresponding Author, P. Stamatopoulos stamatopoulos@certh.gr

[5] Luo H, Wang X, Liu X, Yi L, Wu X, Yu X, Ouyang Y, Liu W and Xiong Q 2023 Machine learning based prediction of biomass pyrolysis with detailed reaction kinetics for thermally-thick particles: from 1D to 0D *Chem. Eng. Sci.* **280** 119060
[6] Yu H and Wilamowski B M 2018 Levenberg–marquardt training *Intelligent systems* (CRC Press) pp 12-1-12–6
[7] Nikolopoulos A, Papafotiou D, Nikolopoulos N, Grammelis P and Kakaras E 2010 An advanced EMMS scheme for the prediction of drag coefficient under a 1.2MWth CFBC isothermal flow—Part I: Numerical formulation *Chem. Eng. Sci.* **65** 4080–8

Acknowledgments

Financial support is acknowledged from the RFCS project of the European Commission under Grant Agreement No. 101034024 (Retrofitting Existing Fluidized Bed Power Plants for Waste-Derived Fuels and CO2 Capture - REBECCA).

*Corresponding Author, P. Stamatopoulos stamatopoulos@certh.gr